© 2017. Published by The Company of Biologists Ltd | Journal of Cell Science (2017) 130, 4155-4167 doi:10.1242/jcs.211102

RESEARCH ARTICLE

CREB3L1-mediated functional and structural adaptation of the secretory pathway in hormone-stimulated thyroid cells

Iris A. García[1], Vanina Torres Demichelis[1], Diego L. Viale[2], Pablo Di Giusto[1], Yulia Ezhova[3], Roman S. Polishchuk[3], Luciana Sampieri[1], Hernán Martinez[1], Elizabeth Sztul[4] and Cecilia Alvarez[1,*]

ABSTRACT

Many secretory cells increase the synthesis and secretion of cargo proteins in response to specific stimuli. How cells couple increased cargo load with a coordinate rise in secretory capacity to ensure efficient transport is not well understood. We used thyroid cells stimulated with thyrotropin (TSH) to demonstrate a coordinate increase in the production of thyroid-specific cargo proteins and ER–Golgi transport factors, and a parallel expansion of the Golgi complex. TSH also increased expression of the CREB3L1 transcription factor, which alone caused amplified transport factor levels and Golgi enlargement. Furthermore, CREB3L1 potentiated the TSH-induced increase in Golgi volume. A dominant-negative CREB3L1 construct hampered the ability of TSH to induce Golgi expansion, implying that this transcription factor contributes to Golgi expansion. Our findings support a model in which CREB3L1 acts as a downstream effector of TSH to regulate the expression of cargo proteins, and simultaneously increases the synthesis of transport factors and the expansion of the Golgi to synchronize the rise in cargo load with the amplified capacity of the secretory pathway.

KEY WORDS: Membrane traffic, Golgi, Secretory pathway, CREB3L1, FRTL-5, TSH

INTRODUCTION

Secretion is essential and occurs in all cells, but the levels vary dramatically. While secretion is modest in many cell types, specialized secretory cells such as those in the pancreas, mammary and salivary glands, synthesize and secrete milligrams of proteins daily. Such cells must adapt to high secretory demand and increase their capacity to synthesize, fold, modify and traffic cargo proteins through the secretory pathway. The upregulation of secretory capacity is usually triggered by developmental or differentiation cues or through physiological stimulation. One of the key questions is how cells coordinate their responses to increase cargo protein expression and at the same time amplify the function and architecture of the secretory pathway to accommodate the increased cargo load.

[1]Centro de Investigaciones en Bioquímica Clínica e Inmunología (CIBICI-CONICET), Departamento de Bioquímica Clínica, Facultad de Ciencias Químicas, Universidad Nacional de Córdoba, Córdoba 5000, Argentina. [2]Laboratorio de Neuro y Citogenetica Molecular, Centro de Estudios en Salud y Medio Ambiente, Escuela de Ciencia y Tecnologiá–Universidad Nacional de San Martiń–CONICET, Buenos Aires, B1650 WAB, Argentina. [3]Telethon Institute of Genetics and Medicine (TIGEM), Via Campi Flegrei, 34, 80078, Pozzuoli (NA), Italy. [4]Department of Cell, Developmental and Integrative Biology, University of Alabama at Birmingham, Birmingham, AL 35233-2008, USA.

*Author for correspondence (calvarez@fcq.unc.edu.ar)

D.L.V., 0000-0003-3061-0590; C.A., 0000-0001-9135-7272

Received 15 September 2017; Accepted 11 October 2017

A well-studied control system within the secretory pathway responds to the level of unfolded proteins within the endoplasmic reticulum (ER) (Ron and Walter, 2007). In this system, increased synthesis of cargo proteins saturates the folding ability of ER chaperones, leading to an accumulation of unfolded proteins and the induction of the unfolded protein response (UPR). Activation of the UPR induces a transcriptional program that causes increased synthesis of folding proteins that raise the folding capacity of the ER and thus relieve ER stress.

Another important, but less-studied homeostatic pathway is related to the adaptation of the Golgi complex in response to high secretory demand. In this system, an increased transport of KDEL-bearing proteins to the Golgi activates the KDEL receptor 1 (KDELR1). The activated KDELR1 initiates a signaling cascade that results in the activation of kinases Src and protein kinase A (PKA), which subsequently upregulate anterograde and retrograde transport, respectively. Importantly, activated PKA mediates the activation of the cAMP-response element-binding protein 1 (CREB1), as well as other cAMP- and non-cAMP-regulated transcription factors (Cancino et al., 2014). CREB1 has been shown to control the transcription of a number of genes that mediate multiple cellular processes, including those that regulate membrane traffic (Romero et al., 2013; Shaywitz and Greenberg, 1999). Moreover, members of the CREB3 subfamily of CREB-like membrane-bound bZIP transcription factors were shown to regulate numerous genes involved in the homeostasis of the secretory pathway, including ER chaperones and various transport factors (Bailey and O'Hare, 2007; Barbosa et al., 2013; Fox et al., 2010; Murakami et al., 2009).

The CREB3 subfamily is highly conserved from sponges to humans (Barbosa et al., 2013), and in mammals is represented by five members known as CREB3 (also LZIP or Luman), CREB3L1 (OASIS), CREB3L2 (BBF2H7), CREB3L3 (CREB-H) and CREB3L4 (AIbZIP). The expression patterns of these proteins is tissue dependent and results in cell type-specific activation of their target genes. The CREB3 subfamily has been implicated in cell differentiation, inhibition of cell proliferation, regulation of development, metabolism and in the upregulation of the core components of the secretory pathway during development (Chan et al., 2011; Fox and Andrew, 2015). However, it remains unknown whether these transcription factors act in an analogous manner in all secretory cells and also regulate the adaptation of the secretory pathway in response to a physiological hormonal stimulation.

In this study, we used an inducible secretory cellular model based on a thyroid cell line (FRTL-5) to study the response of the secretory pathway to hormonal stimulation. In these cells, exogenously added thyroid-stimulating hormone (TSH) or thyrotropin, interacts with its cell surface receptor (TSH-R) and initiates a cAMP-signaling cascade resulting in synthesis of thyroid-specific proteins that traffic through the secretory pathway to reach their destinations. The

Journal of Cell Science (2017) 130, 4155-4167 doi:10.1242/jcs.211102

FRTL-5 system was used to study the effects of TSH stimulation on the synthesis of thyroid-specific cargo proteins such as thyroglobulin (Tg) and the sodium-iodide symporter (NIS, also known as SLC5A5), the synthesis of secretory pathway components (transport factors), and the changes in size and structure of the Golgi complex.

We report that TSH-induced signaling pathways coordinately increased the expression of a thyroid-specific cargo protein and transport factors, and amplified the size of the Golgi complex. We determined that TSH stimulated the expression of the CREB3L1 transcription factor, and that CREB3L1 alone induced a marked increase in Golgi volume. Furthermore, levels of a representative transport factor (Rab1b) increased in CREB3L1-overexpressing cells and decreased when CREB3L1 expression was inhibited by shRNA treatment. Our results suggest that a physiologically appropriate stimulation of specialized secretory cells triggers signaling circuits that coordinately regulate the synthesis of tissue-specific cargo proteins and ubiquitous molecules that regulate the structure and function of the secretory pathway, and cause a synchronous expansion of a key secretory compartment, the Golgi complex.

RESULTS

TSH stimulation of thyroid cells increases expression of transport factors

We have shown previously that treatment of FRTL-5 thyroid cells with TSH increases the expression of two Golgi proteins, Rab1b and GM130 (also known as GOLGA2) (Romero et al., 2013), known to facilitate secretory trafficking at the ER–Golgi interface. This raised the possibility that TSH stimulation may have a general effect on the regulation of the secretory pathway and may also increase the expression of other ubiquitous transport factors. Thus, we assessed the levels of additional proteins required for secretory membrane traffic (transport factors) that localize to and function in different secretory compartments in FRTL-5 cells grown in basal medium [without (−)TSH] for ∼72 h, and then induced with TSH (for 24 h, see Materials and Methods for further details). Calreticulin was used as a representative chaperone in the ER, while Sec16a and Sec23a function at ER exit sites (ERES) sequestering cargo into COPII transport vesicles for export from the ER (Fromme et al., 2008). GBF1 and Arf1 represent factors required for the formation of COPI vesicles that mediate recycling of proteins from the Golgi to the ER (Szul and Sztul, 2011). GM130, p115 (also known as USO1), Rab1b and Golgin 97 (also known as GOLGA1) are all transport factors that localize to and function at the Golgi (Sztul and Lupashin, 2009). As shown in Fig. 1A, all assayed transport factors were observed at their expected subcellular localizations in cells cultured under basal conditions (−TSH). Upon TSH stimulation, an increase in immunofluorescence intensity was observed for all proteins, suggesting that there is an increase in their protein levels, which was confirmed by western blot analysis (Fig. 1B). NIS was used as a positive control for stimulation, and shows an extensive increase in levels in TSH-treated cells. All transport factors were detectable in cells cultured under basal conditions, but densitometry analysis indicated that most of them exhibited a significant increase after TSH stimulation (Fig. 1C). GM130, Rab1b and p115 exhibited the highest increase in expression levels after TSH stimulation (∼3.0-, ∼2.9- and ∼2.5-fold, respectively). GAPDH was used as a loading control since its expression is not induced by TSH.

To test whether the increases in protein levels correlated with increased transcription, we assessed the mRNA levels of GM130 and Rab1b by real-time quantitative reverse transcription PCR (qRT-PCR). The NIS mRNA level was analyzed as a positive control for TSH-induced transcriptional upregulation. In agreement with the western blot data, the mRNA levels of GM130 and Rab1b in TSH-stimulated cells were higher than in cells grown under basal conditions (∼1.5-fold for GM130 and ∼2.5-fold for Rab1b, Fig. 1D). In addition, we evaluated the mRNA levels of two other transport factors, the Sec31a component of the COPII coat required for ER to Golgi transport (Hughes and Stephens, 2008) and the KDELR3 receptor involved in retrograde retrieval of KDEL-tagged proteins from the Golgi to the ER, a process essential for repeated rounds of ER–Golgi transport (Capitani and Sallese, 2009). As shown in Fig. 1D, mRNA levels increased ∼2.5-fold for Sec31a and ∼1.5-fold for KDELR3. Taken together, our results indicate that TSH regulates expression of thyroid-specific proteins (i.e. NIS), as well as numerous transport factors required for membrane trafficking through the secretory pathway.

Timecourse of TSH-induced changes in transport factor protein and mRNA levels

Previous studies in FRTL-5 cells have shown that immediately after TSH stimulation, ER chaperones and folding enzymes exhibit the maximum rates of synthesis, followed by thyroid-specific proteins (Christis et al., 2010). This suggests that the increase in the folding capacity of the ER occurs before the accumulation of thyroid-specific proteins in the ER, thus preventing the UPR. The relationship between the upregulation of thyroid-specific proteins and the adaptation of the secretory pathway is not well understood. Therefore, we compared the kinetics of the TSH-induced increase in a thyroid-specific cargo protein (NIS) relative to a number of transport factors. FRTL-5 cells were stimulated with TSH for varying length of time and the levels of NIS and transport factors were assessed by western blot analysis. As shown in Fig. 2A,B, NIS was undetectable after 4 h of TSH stimulation, and was barely detected after 8 h of TSH. Because NIS was not detected after 0 or 4 h of TSH treatment, the NIS level at 8 h was considered basal to calculate fold changes at the other time points. A significant increase in the amount of NIS was observed after 14 and 24 h of TSH stimulation. The kinetics of NIS expression after TSH induction are similar to those reported for another thyroid-specific cargo, thyroglobulin [Tg (Christis et al., 2010)].

Increases in protein levels after TSH stimulation were observed for all tested transport factors (Fig. 2A,B). Calreticulin, calnexin and GM130 showed significant increases (∼3-fold) after 8 h, and remained roughly at the same level up to 24 h. Rab1b showed a significant increase (∼3-fold) after 14 h and continued to increase (∼5-fold) 24 h after TSH stimulation. Although the Arf1 immunofluorescence signal in TSH-treated cells was higher than in control cells (Fig. 1A), its protein levels showed only a minor increase. This difference could be due to increased Arf1 activation and consequent membrane association without a major increase in total amount of Arf1. In agreement with this possibility, higher levels of GBF1, an exchange factor for Arf1 at the ER–Golgi interface (Garcia-Mata et al., 2003) was detected in TSH-treated cells (Fig. 1B, C). In contrast, the levels of the GTPase Rab1b increased significantly in response to TSH, suggesting that different regulation pathways modulate the demand for the activity of this GTPase. Importantly, all examined proteins (cargo and transport factors) were induced in response to TSH, suggesting a similar regulatory control.

To assess whether transcriptional changes could underlie the increased protein levels, we compared mRNA levels of cargo proteins (NIS and Tg) and a transport factor (Rab1b) at different

Journal of Cell Science (2017) 130, 4155-4167 doi:10.1242/jcs.211102

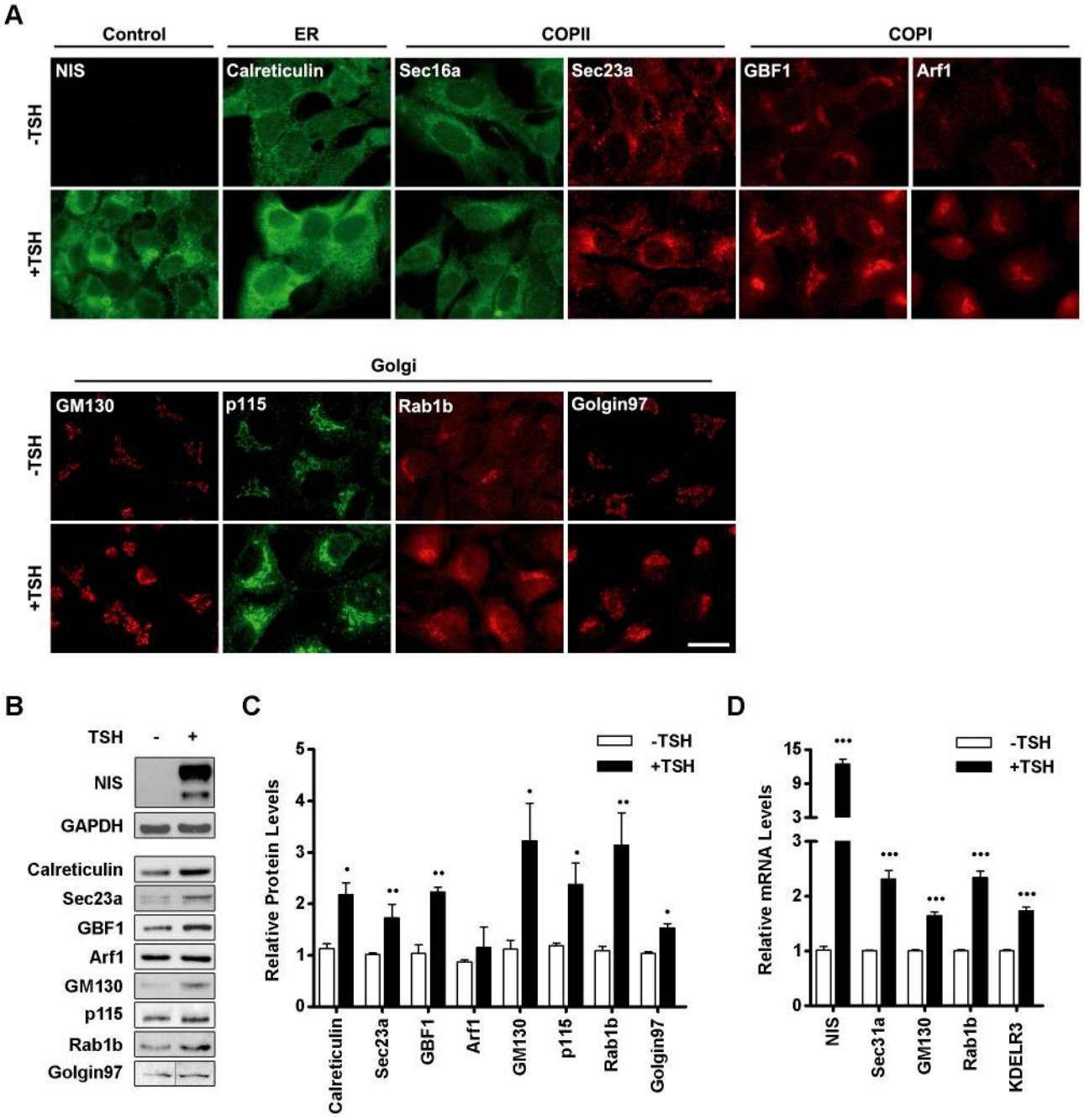

Fig. 1. Transport factors are upregulated in response to TSH stimulation. (A) Immunofluorescence staining of the indicated transport factors performed on FRTL-5 cells grown under basal (−TSH) conditions or cells treated with TSH (+TSH, 1 mIU/ml, 24 h). NIS was used as positive control for induction. Images are representative of three independent experiments. Scale bar: 10 µm. (B) Western blot analysis of lysates from FRTL-5 cells incubated under basal (−TSH) or stimulated (+TSH, 1 mIU/ml, 24 h) conditions. NIS and GAPDH were used as controls for TSH induction and loading, respectively. (C) Densitometric quantification of proteins shown in B normalized to GAPDH. Values represent fold change relative to protein levels under basal conditions (see Materials and Methods). Bar graph represents mean±s.e.m. of at least three independent experiments (*P<0.05; **P<0.01). (D) Quantification of transport factors mRNA by qRT-PCR from total RNA obtained from FRTL-5 cells grown under basal (−TSH) or stimulated (+TSH, 1 mIU/ml, 14 h) conditions. NIS was used as positive control of TSH induction. Results were normalized to the levels of β-actin and expressed according to the $2^{-\Delta\Delta Ct}$ method relative to the expression level in basal conditions (set as 1). Results are mean±s.e.m. of at least three independent experiments performed in triplicate (***P<0.001).

time points after TSH stimulation by performing qRT-PCR. As shown in Fig. 2C, NIS mRNA levels increased significantly (~4-fold) within the first 4 h and continued to increase to ~5-fold at 6 h and ~9-fold at 14 h post TSH stimulation. The increases in Tg mRNA are also significant, but less pronounced with a ~1.5-fold increase at 4 h, a ~2.5-fold increase at 6 h and a ~2-fold at 14 h after TSH stimulation. The kinetics and the extent of Tg induction are closely matched by the kinetics of Rab1b induction: Rab1b mRNA increases ~2-fold at 4 h, continues to increase to ~2.5-fold at 6 h followed by a slight drop to ~2-fold at 14 h. Thus, it appears that the TSH-induced increase in cargo (NIS and Tg) production is paralleled by an increase in secretory capacity (Rab1b), suggesting that the same pathway may upregulate the synthesis of cargo and transport factors.

Journal of Cell Science (2017) 130, 4155-4167 doi:10.1242/jcs.211102

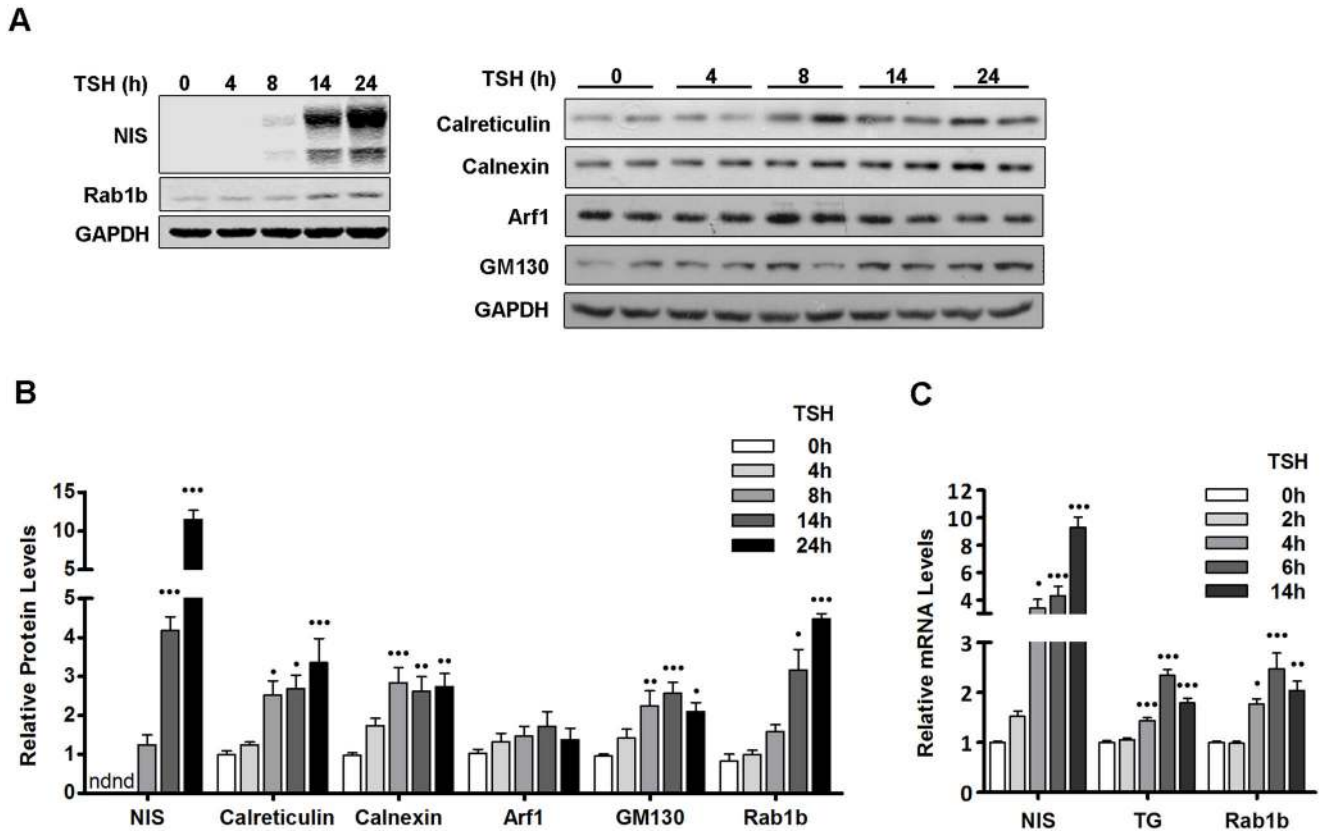

Fig. 2. Cargo proteins and transport factors display similar kinetics of expression in response to TSH stimulation. (A) Western blot of lysates from FRTL-5 cells stimulated with TSH (1 mIU/ml) for the indicated times. NIS was used as positive control for TSH induction, and GAPDH as a loading control. (B) Densitometric quantification of proteins in A normalized to GAPDH. Values represent fold change relative to protein levels at 0 h (see Materials and Methods). Results are mean±s.e.m. of at least three independent experiments. nd, not detectable (*P<0.05; **P<0.01; ***P<0.001). (C) Quantification of mRNA levels by qRT-PCR with total RNA obtained from FRTL-5 cells stimulated with TSH (1 mIU/ml) for the indicated times. Results were normalized to β-actin and expressed according to the $2^{-\Delta\Delta Ct}$ method relative to the expression level at 0 h (set as 1). Results are mean±s.e.m. of three independent experiments performed in triplicate (*P<0.05; **P<0.01; ***P<0.001).

TSH stimulation of thyroid FRTL-5 cells increases Golgi size and volume

The TSH-induced increase in levels of transport factors is likely to represent a physiological response of thyroid cells to adapt the secretory pathway for high transport. It has been reported that the size and volume of the Golgi complex increase or decrease in response to secretory demand (Sengupta and Linstedt, 2011). For example, an extreme expansion of the Golgi has been described in the lactating mammary gland, where the number and size of Golgi cisterna increased dramatically during the secretion of milk (Clermont et al., 1993; Sinowatz et al., 1980). Thus, we examined the effect of TSH treatment on Golgi complex morphology in FRTL-5 cells at different times after TSH addition. We monitored the Golgi complex by assessing the localization of GM130, a marker for the *cis*-Golgi, and of the glucosyl-transferase GalNacT$_2$ (also referred as GALNT2) that localizes to the *medial*- and *trans*-Golgi cisterna (Rottger et al., 1998). Confocal microscopy was used to acquire *z*-stack images of GM130 and GalNacT$_2$. As shown in Fig. 3A for GM130 and Fig. 3C for GalNacT$_2$, the Golgi enlarged significantly during TSH treatment: clear differences were observed after 14 h, and even more dramatic effects were seen after 24 h of TSH treatment. To further analyze morphological changes, we used the Huygens Essential software to assess Golgi volume by 3D reconstruction after the deconvolution of *z*-stacks (Fig. 3B,D). Quantification of Golgi volume shows that it increases by ∼3- to ∼4-fold after 14 and 24 h of TSH stimulation, respectively (Fig. 3E, F). Importantly, similar increases were observed when Golgi complex was monitored with the *cis* marker GM130 and the *medial*- and *trans*-Golgi marker GalNacT$_2$, suggesting that all compartments of the Golgi complex underwent enlargement in response to higher secretory demand.

To understand the structural modifications responsible for the increase in Golgi volume, we used transmission electron microscopy (EM) to quantify the number of cisternae within the stack as well as the stack length in untreated FRTL-5 cells and in cells treated with TSH for 24 h (30 individual stacks were analyzed). As shown in representative images in Fig. 3G–I, the Golgi stacks show an increase in the number of cisterna and their length after TSH stimulation. Quantification indicates that, in TSH-treated cells, the number of cisterna per Golgi stack increases by one or two, with a concomitant increase in stack length (Fig. 3J). In addition, in TSH-treated cells, we observed regions of cisternae with distended lumens (Fig. 3I). Distended cisternae containing collagen aggregates are often seen in collagen-secreting cells (Bonfanti et al., 1998; Trucco et al., 2004). Thus, distended cisternae appear to be linked to an increased amount of cargo protein(s) moving through the Golgi complex. We assume that this is the case for TSH-treated cells. Taken together, our biochemical and morphological analysis suggest that the TSH induces increases in the synthesis of thyroid specific cargo (e.g. NIS) and ubiquitous transport factors (e.g. Rab1b, p115 and GM130), as

Journal of Cell Science (2017) 130, 4155-4167 doi:10.1242/jcs.211102

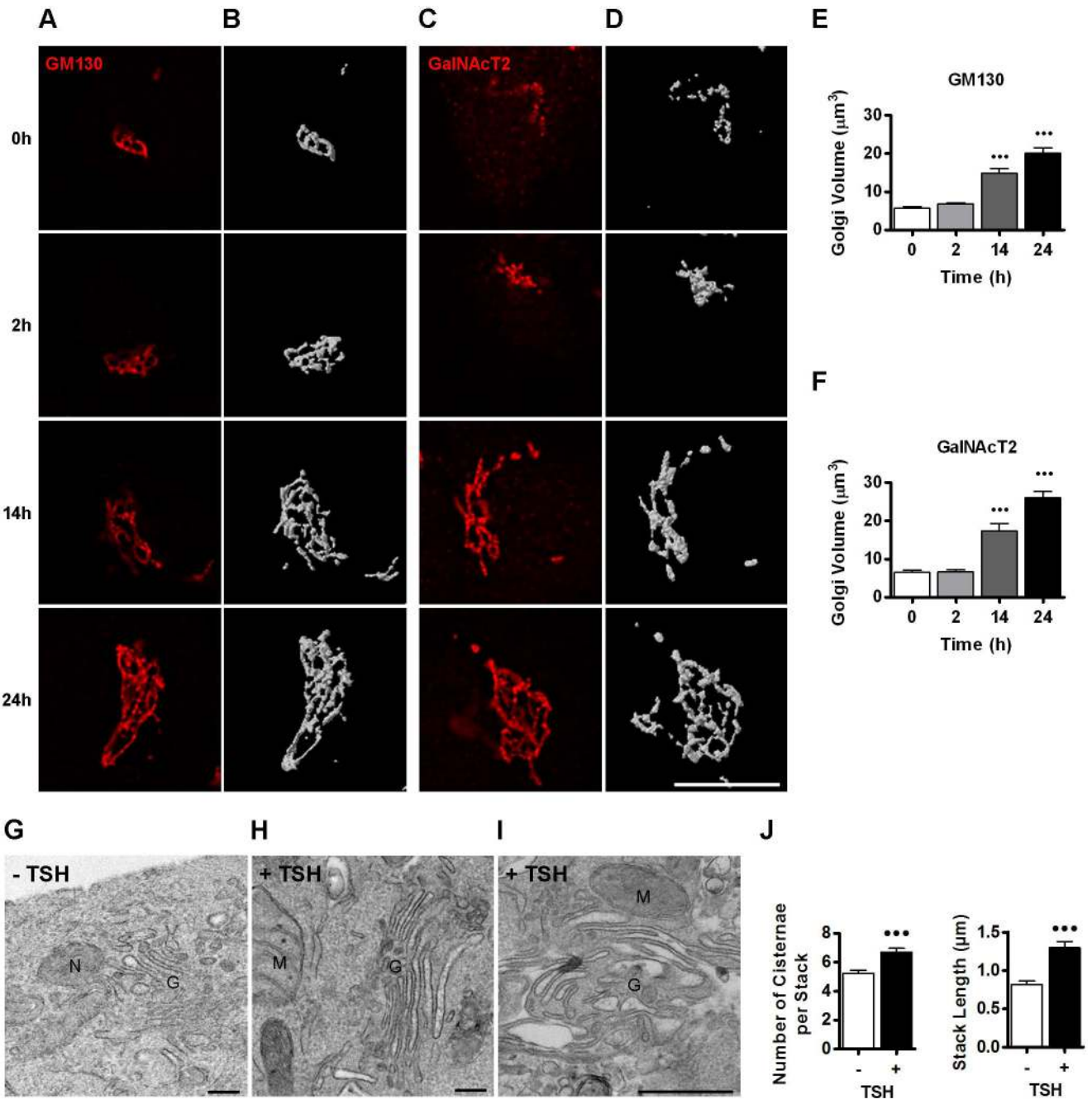

Fig. 3. TSH stimulation leads to increased Golgi size and volume. (A,C) Deconvolved images obtained from immunofluorescence analysis performed on FRTL-5 cells with antibodies against GM130 (A) and GalNAcT2 (C) at the indicated time points after TSH stimulation. (B,D) Three-dimensional reconstruction of the images shown in A and C, respectively. Scale bar: 10 µm. (E,F) Quantification of Golgi volume normalized to cell size. Cell size was estimated by flow cytometry and the average size of the cell population at 0 h was set as 1. Results are mean±s.e.m. of two independent experiments with 14–17 cells analyzed per condition (***P<0.001). (G–I) Electron micrographs of FRTL-5 cells incubated under basal (−TSH) conditions (G) or after TSH stimulation (+TSH, 1 mIU/ml) for 24 h (H,I). Images are representative of two independent experiments. N, nucleus; M, mitochondria; G, Golgi. Scale bars: 300 nm. (J) Quantification of number of cisternae within a single stack and stack length for each condition (−TSH or +TSH, 30 stacks were counted in different cells, ***P<0.001, t-test).

well as causing the expansion of the Golgi complex. This suggests a coupled induction program that ensures coordination of cargo production with the adaptation of the secretory pathway to handle the transport of such cargo.

Forskolin mimics the TSH-induced increase in the expression of transport factors

TSH is known to mediate its stimulatory effect on the expression of thyroid-specific proteins by activating the cAMP pathway (Dremier et al., 2002). The interaction of TSH with its receptor, TSH-R, a member of the G protein-coupled receptor family, activates the G_s and G_q subunits of the heterotrimeric G proteins (Morshed et al., 2009). Activated G_s largely mediates its action through inducing an increase in adenylate cyclase activity, leading to a raise in intracellular cAMP, which in turn activates the CREB proteins. Importantly, the TSH stimulatory effect can be replicated by treating cells with forskolin [a pharmacological agent that increases cellular cAMP levels by directly activating adenylate cyclase (Seamon et al.,

Journal of Cell Science (2017) 130, 4155-4167 doi:10.1242/jcs.211102

1981)]. To explore whether a cAMP-responsive element may mediate the increased expression of transport factors in TSH-treated cells, we compared the effects of TSH and forskolin on the expression of a thyroid-specific cargo protein (NIS) and a set of transport factors (calreticulin, Sec23a, GM130 and Rab1b). FRTL-5 cells were stimulated with either TSH or forskolin and the levels of each protein were assessed by performing western blotting. As expected, the increase in the level of NIS after stimulation with forskolin was similar to that observed after TSH treatment (Fig. 4A,B). Importantly, the levels of calreticulin, Sec23a and GM130 also showed similar levels of induction when cells were stimulated with forskolin or TSH (Fig. 4A,B). The intensity of the response to TSH was slightly lower than that shown in Fig. 1, most likely due to inherent cell variability and differences in the biological activity of the reagents (especially TSH). However, the overall increases in the response to TSH were maintained and, in experiments performed in parallel, stimulation with forskolin caused a response that was similar to that after TSH treatment. These results indicate that the TSH-mediated increase in transport factors operates through a pathway analogous to that used to induce NIS expression, and that both are mediated by a cAMP signaling pathway and CREs.

To find overrepresented motifs in the promoter region of genes coding for transport factors, the WebMOTIFS (Romer et al., 2007) and Pscan (Zambelli et al., 2009) online motif discovery software were used. We compared the sequences of promoter regions of 36 genes (Table 1). A total of 34 were transport factors, including 28 genes modified in Rab1b-overexpressing cells (Romero et al., 2013); four genes encoded proteins upregulated by TSH (ARF1, GBF1, SEC23A, RAB1B), and two encoded Rab family members (RAB5A and RAB7A). In addition, calreticulin and GalNAcT were selected as ER and Golgi representatives, respectively. WebMOTIFS revealed a single motif that was overrepresented by 8-fold and was similar to the consensus motif for CREB/ATF response elements (data not shown). In agreement, Pscan software identified the CREB3L1 motif (Fig. 4C) as among the motifs with the highest *P*-value (CREB3L1 Bonferroni-corrected $P=8.38\times10^{-8}$) and the most enriched compared to a random selection of 36 promoters (Welch's *t*-test $P=1.06\times10^{-4}$) in the sequences analyzed. As expected, this sequence is similar to the consensus motif for CREB/ATF response elements, and agrees with a previous study in *Drosophila* showing that this consensus sequence is present in the regulatory region of genes coding for secretory pathway components activated by CrebA (Abrams and Andrew, 2005).

TSH induces the expression of the CREB3L1 transcription factor

The presence of CRE sequences in the promoter region of transport factors and the higher mRNA levels of transport factors in response to increased intracellular cAMP suggest that a member of the CREB3 family might be involved in the changes induced by TSH. The human CREB3 family contains five proteins, with CREB3L1 and CREB3L2 being the most similar to the CrebA of *D. melanogaster*, which is known to regulate secretory capacity (Fox et al., 2010). Thus, we explored the effect of TSH on the levels of CREB3L1 and CREB3L2 protein and mRNA. As shown in Fig. 5A,B, the protein levels of CREB3L1 increased in response to TSH in a time-dependent manner, with an ∼2.5-fold increase being seen after 8 h and a ∼3-fold increase at 14 h. In contrast, the levels of CREB3L2 were not significantly changed by TSH. In agreement with the western blot data, qRT-PCR revealed a time-dependent increase in CREB3L1 mRNA with an ∼2-fold increase after 2 h of TSH induction and levels reaching a reaching a maximum of an ∼6-fold increase after 4 h of TSH induction (Fig. 5C). TSH did not significantly influence the levels of CREB3L2 transcripts, in agreement with the protein data. We also measured CREB3 and CREB3L3 mRNA levels by performing a qRT-PCR after 0, 2, 4 and 14 h of TSH stimulation: minimal CREB3 and CREB3L3 mRNA levels were detected at all time points, and their levels were not significantly changed by TSH treatment (Fig. S1). We did not detect an amplification product for CREB3L4 mRNA at any time point when using total RNA from FRTL-5 cells under conditions when we detected the expected size product using RNA from neuronal cells (data not shown). Thus, TSH-mediated stimulation of thyroid FRTL-5 cells appears to selectively upregulate the production of the CREB3L1 transcription factor, suggesting that the TSH-induced adaptation of the secretory pathway is mediated by CREB3L1.

CREB3L1 regulates Rab1b and GM130 expression in FRTL-5 cells

To assess the role of CREB3L1 in regulating the expression of transport factors, we analyzed the effect of CREB3L1

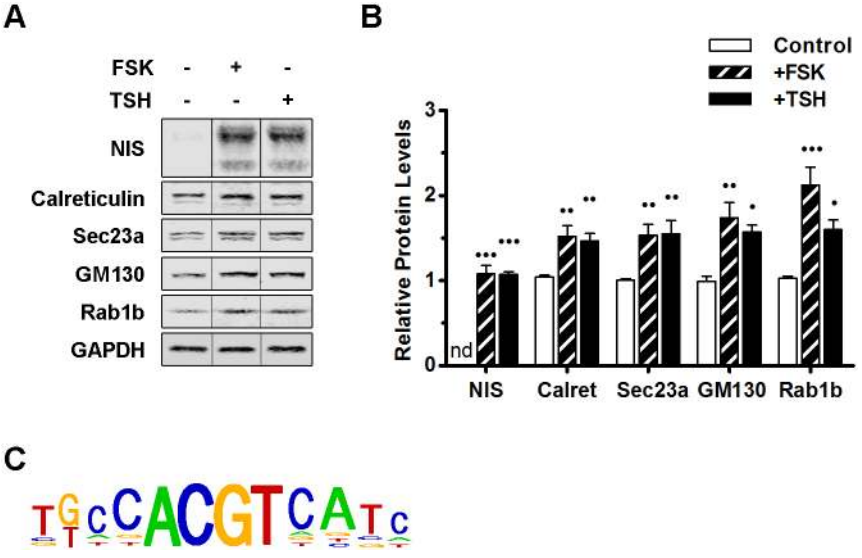

Fig. 4. The cAMP-dependent signaling pathway is responsible for the increases in protein and mRNA levels of transport factors. (A) Western blot of lysates from FRTL-5 cells grown under basal conditions (−FSK/−TSH, control) or treated either with FSK (+FSK, 10 µM) or TSH (+TSH, 1 mIU/ml) for 24 h. NIS and GAPDH were used as controls for TSH induction and loading, respectively. (B) Densitometric quantification of proteins in A normalized to the levels of GAPDH. Values indicate the fold change relative to protein levels in untreated cells. Results are mean±s.e.m. of three independent experiments (*$P<0.05$; **$P<0.01$; ***$P<0.001$). (C) The CREB3L1 consensus motif identified upstream of 36 genes selected as described in the Results (listed in Table 1) as determined by Pscan.

Journal of Cell Science (2017) 130, 4155-4167 doi:10.1242/jcs.211102

Table 1. Analysis of promoter regions

Symbol	Gene name	Position	CREB3L1 homology	Score
ARF1°	ADP ribosylation factor 1	−291	AGGGCACGTCGACC	0.723
ARF4	ADP ribosylation factor 4	−86	GGGCCACGTCCGGG	0.782
ARL1	ADP ribosylation factor-like 1	−343	AGACTACGTAATAA	0.710
BET1	Bet1 Golgi vesicular membrane trafficking protein	25	GCGCCACGACATCA	0.883
CALR°	Calreticulin	−81	CTGCCACTTTGTCA	0.773
COPG1	Coatomer protein complex, subunit γ	−17	TGGCCACGTCGCCC	0.821
COPZ2	Coatomer protein complex, subunit ζ2	−94	GGGCCCCGTCCTCT	0.745
CYTH1	cytohesin 1 Pleckstrin homology, Sec7 and coiled-coil domains 1 PSCD1	−446	AGGCCACAAAAGCT	0.706
GALNT2 (GalNAcT2)°	N-acetylgalactosaminyltransferase 2	−235	CTGCCGCGTCTCCA	0.835
GBF1°	Golgi brefeldin A resistant guanine nucleotide exchange factor 1	36	TTACCACGTCAGTG	0.826
GEM	GTP binding protein overexpressed in skeletal muscle	−276	GTGACACTTAATCG	0.787
GOLGA1	Golgi autoantigen, golgin subfamily a, 1	−162	TCGCCACGTCAGCG	0.907
GOLGA2 (GM130)°,+	Golgi autoantigen, golgin subfamily a, 2	8	GGGCCACATCAGCG	0.821
GOLGA3	Golgi autoantigen, golgin subfamily a, 3	−161	CGGCCACGTCTCCG	0.835
GORASP2	Golgi reassembly stacking protein 2, 55 kDa	11	TAGCCAGGTCGTAT	0.716
KDELR3+	KDEL endoplasmic reticulum protein retention receptor 3	−15	TGGCCACGTCACCG	0.884
NAPA	N-ethylmaleimide-sensitive factor attachment proteinα	−23	CTCCCACGTGACCC	0.790
RAB11FIP2	RAB11 family interacting protein 2 (class I)	−392	TCGCCACGGCAACC	0.786
RAB1B°,+	Rab1b	−423	GCCGCGCGTCATCA	0.693
RAB26	RAB26, member RAS oncogene family	−140	CTGCCACAGCGACT	0.723
RAB32	RAB32, member RAS oncogene family	36	ACGCCGCCTGACCG	0.701
RAB5A	Rab5a	30	CCGCCACGTCGCTG	0.835
RAB7A	Rab7a	−238	ATGCCACCGAAGAG	0.699
RABAC1	Rab acceptor 1 (prenylated)	−19	GCGCCACGTCGACT	0.854
RHOBTB3	Rho-related BTB domain containing 3	−259	TTACCACGTCTGCC	0.795
RRAGC	Ras-related GTP binding C	−60	GTGCCCCGTCACGT	0.808
SEC22L1	SEC22 vesicle trafficking protein-like 1	−4	CGGCCACCTCAGCG	0.795
SEC23A	Sec23 homolog A, coat complex II component	−9	CTGCCACGTCAAGA	0.910
SEC24D	SEC24 related gene family, member D	−193	TAGCCACGACGTTA	0.757
SEC31A+	SEC31 homolog A	−253	ACGCCACGTAGCAC	0.792
SERP1	Stress-associated endoplasmic reticulum protein 1	−105	CCTACACGTCTCCT	0.744
SRP54	Signal recognition particle 54 kDa	26	GTGCCCCGGAAGCG	0.728
STX3A	Syntaxin 3A	−259	GAGAAACGTAAGCA	0.749
STXBP1	Syntaxin binding protein 1	11	CTGCCCCGCCGCCG	0.714
USO – VDP (p115)	Vesicle docking protein p115 - USO1 vesicle transport factor	−246	CTGTCACGTTGGCC	0.716
YIF1A	Yip1 interacting factor homolog (*S. cerevisiae*)	−247	CTGCCACGACTACA	0.820

Promoter sequences (from −450 to +50 relative to the transcription start site) of the indicated genes were analyzed by Pscan software. The CREB3L1 consensus motif displayed was enriched compared to a random selection (see Results for details). Individual putative CREB3L1 sites and score are shown. Genes analyzed by western blotting or/and immunofluorescence are indicated with a '°', while genes analyzed by qRT-PCR are indicated with a '+'.

overexpression on Rab1 levels. A limitation of the FRTL-5 cell system is that they are not easy to transfect (their transfection efficiency fluctuate between 5 to 15%). Therefore, to obtain an enriched population of CREB3L1-overexpressing cells, we co-transfected FRTL-5 cells with CREB3L1FL and the pLKO.1 vector (ratio 1:3), which confers resistance to puromycin. As a control, we used FRTL-5 cells transfected with pLKO.1 alone. After 30 days of puromycin selection, the cells transfected with both

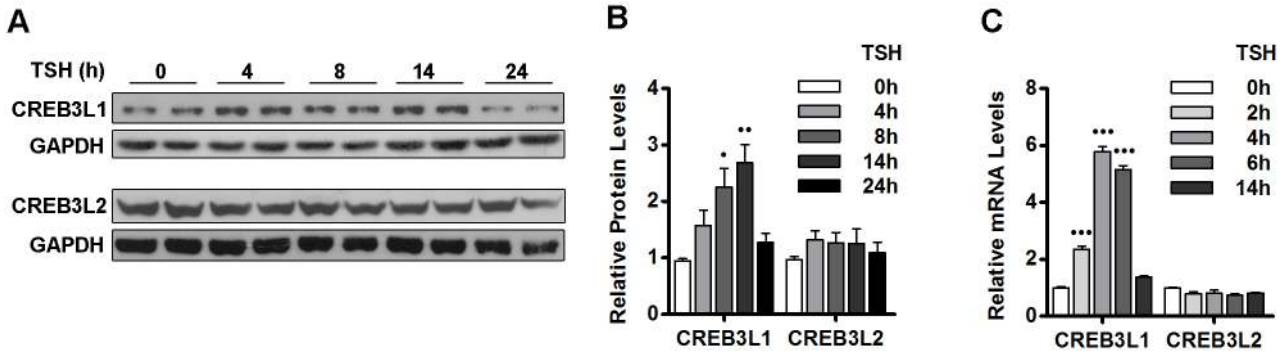

Fig. 5. TSH stimulates CREB3L1 expression. (A) Western blot with antibodies against the N-terminal region of CREB3L1 or CREB3L2 in lysates from FRTL-5 cells stimulated with TSH (1 mIU/ml) for the indicated times. GAPDH was used as the loading control. (B) Densitometric quantification of proteins in A normalized to the levels of GAPDH. Values are the fold change relative to levels in cells at 0 h. Results are mean±s.e.m. of three independent experiments (*P<0.05; **P<0.01). (C) Quantification of CREB3L1 and CREB3L2 mRNA levels by qRT-PCR performed with total RNA from FRTL-5 cells stimulated with TSH (1 mIU/ml) for the indicated times. Results are normalized to the levels of β-actin, expressed according to the $2^{-\Delta\Delta Ct}$ method relative to levels at 0 h (set as 1) and are shown as mean±s.e.m. of three independent experiments performed in triplicate (***P<0.001).

Journal of Cell Science (2017) 130, 4155-4167 doi:10.1242/jcs.211102

CREB3L1FL and pLKO.1, were analyzed for expression of CREB3L1 by performing immunofluorescence microscopy. As shown in Fig. 6A, ∼50% of the puromycin-resistant cells exhibited high levels of CREB3L1. The cells transfected with pLKO.1 alone did not show any signal when probed with anti-CREB3L1 through immunofluorescence (data not shown). Control and CREB3L1-expressing cells were western-blotted to assess the levels of CREB3L1 and the Rab1b transport factor. As shown in Fig. 6B, overexpression of CREB3L1 (∼2.5-fold relative to the control) increased Rab1b levels ∼3.5-fold, indicating that expression of CREB3L1 alone is sufficient to increase Rab1b levels.

The puromycin-selected CREB3L1-overexpressing cells were subsequently used to assess the effect of CREB3L1 depletion on the levels of transport factors. The cells were transiently transfected with a commercial pGFP-C-shLenti vector designed to inhibit CREB3L1 expression. As a control, cells were transfected with an analogous vector containing an shRNA control cassette. Cells were grown for ∼72 h to allow silencing, and then subjected to fluorescence-activated cell sorting (FACS) to isolate GFP-expressing cells. CREB3L1 levels were assessed by western blotting and quantified relative to tubulin, as a loading control. As shown in Fig. 6C, the levels of CREB3L1 in cells expressing the vector designed to inhibit CREB3L1 expression were ∼50% less than in the control cells. Importantly, CREB3L1-depleted cells showed decreased expression of GM130 and Rab1b (∼25% and ∼50%, respectively) relative to that in the control cells (Fig. 6C). Taken together, our results show that the increase or the decrease in the levels of CREB3L1 in thyroid cells affects the expression of endogenous Rab1b and GM130. This suggests that the mechanisms that regulate expression of transport factors are sensitive to changes in CREB3L1 levels, and that, in thyroid cells, CREB3L1 facilitates the adaptation of the secretory pathway to increase secretory capacity.

CREB3L1 mediates the expansion of the Golgi complex

Since TSH stimulation of FRTL-5 cells leads to a dramatic increase in Golgi volume at the time that CREB3L1 expression is significantly upregulated, we tested the role of CREB3L1 in Golgi expansion by expressing either the full-length CREB3L1 (CREB3L1FL) or the constitutively active CREB3L1 construct (CREB3L1CA) containing only the N-terminal DNA-binding and transactivation domains. Moreover, we evaluated the effect of a dominant-negative CREB3L1 construct containing the N-terminal fragment but lacking the transactivation domain (CREB3L1DN). The cellular localization of these constructs was analyzed through immunofluorescence microscopy performed using a dilution of the anti-CREB3L1 antibody that allows to differentiate transfected cells from the non-transfected cells. In agreement with previous reports (Murakami et al., 2009; Saito et al., 2014), CREB3L1FL localizes in both, the nucleus and the endoplasmic reticulum, while CREB3CA and CREB3L1DN are mostly nuclear, with some cells showing both, nuclear and ER distribution (Fig. 7A).

Golgi architecture was assessed by immunofluorescence analysis with anti-GM130 antibody in cells transfected with the CREB3L1 constructs for 36 h and treated with TSH for various times. Transfected cells were identified with anti-CREB3L1 antibody. As shown in Fig. 7B,F, control cells started to show an increase in Golgi volume after 4 h and a further increase after 14 h of TSH stimulation. A time-dependent increase in Golgi volume was also observed in cells expressing the CREB3L1FL (Fig. 7C,F) and the CREB3L1CA construct (Fig. 7D,F). Importantly, in cells expressing the CREB3L1FL or the CREB3L1CA, Golgi volume was significantly increased (more than ∼2-fold) compared to control cells even before TSH stimulation (0 h, Fig. 7F). Stimulation for 2, 4 or 14 h further amplified the differences in the Golgi volume of control cells versus cells expressing the full-length or the constitutively active CREB3L1 construct (Fig. 7F). In contrast, the expression of the CREB3L1DN did not show a significant increase in Golgi volume at any time point (Fig. 7E,F). The fact that CREB3L1DN expression did not modify the Golgi volume indicates that the increases observed with CREB3L1FL and CREB3L1CA were not just a consequence of overexpression. Thus, our results show that the expression of a functional CREB3L1 can increase the volume of the Golgi complex in the absence of TSH stimulation, and that CREB3L1 strongly potentiates the TSH response.

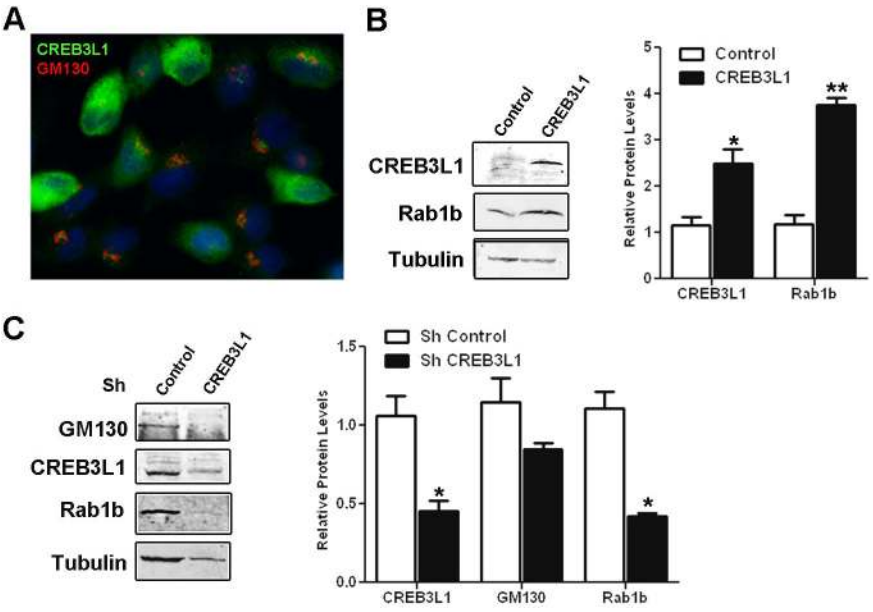

Fig. 6. CREB3L1 regulates Rab1b and GM130 expression. (A) Immunofluorescence analysis with antibodies against CREB3L1 (green) and GM130 (red) of FRTL-5 cells co-transfected with CREB3L1 and the puromycin-resistance conferring pLKO.1 plasmid after selection with puromycin. Nuclei are labeled with Hoechst 33258. (B) Left, western blot of lysates from puromycin-resistant FRTL-5 cells transfected with only pLKO.1 (Control) or co-transfected with pLKO.1 and CREB3L1FL. Tubulin was used as a loading control. Right: densitometric quantification of proteins normalized to the levels of tubulin. (C) Left: western blot of lysates from FRTL-5 cells overexpressing CREB3L1 (cells shown in A) that were transfected with an shRNA containing either a control cassette (control) or CREB3L1-silencing cassette (CREB3L1). Tubulin was used as loading control. Right: densitometric quantification of proteins normalized to the levels of tubulin. Results are mean±s.e.m. of three independent experiments (*P<0.05; **P<0.01).

Journal of Cell Science (2017) 130, 4155-4167 doi:10.1242/jcs.211102

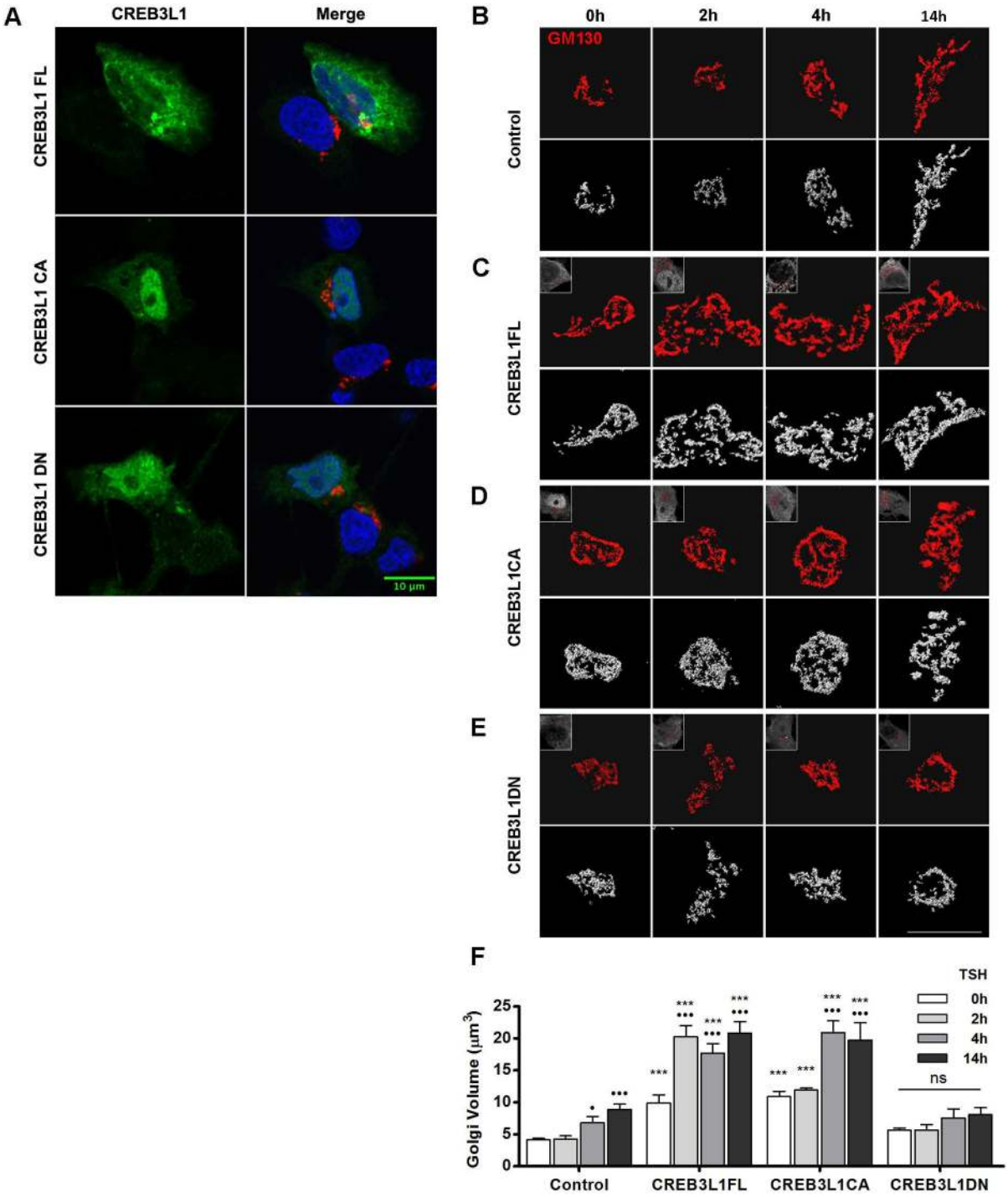

Fig. 7. CREB3L1 induces Golgi expansion and potentiates the TSH-mediated Golgi amplification. (A) Immunofluorescence of FRTL-5 cells transfected with the indicated CREB3L1 construct labeled with antibodies against CREB3L1 (green) and GM130 (red). Nuclei are labeled with Hoechst 33258. FRTL-5 cells were either mock transfected (B; control), or transfected with a full-length CREB3L1 (C; CREB3L1FL), a constitutively active CREB3L1 construct (D; CREB3L1CA), or a dominant-negative CREB3L1 construct (E; CREB3L1DN). After 36 h, cells were stimulated with TSH (1 mIU/ml) for the indicated times and then processed for immunofluorescence analysis with antibodies against CREB3L1 (to identify the transfected cells) and GM130 (to visualize the Golgi). Upper panels, deconvolved images; lower panels, three-dimensional reconstructions of deconvolved images; inset, CREB3L1 expression. Scale bars: 10 µm. (F) Golgi volumes were quantified for each condition at each time point. Results are mean±s.e.m. (*P<0.05; ***P<0.001 versus value at time 0 h for each experimental condition; *P<0.05; ***P<0.001 versus control condition at the same time point); ns, not significant. Spatial deconvolution, three-dimensional reconstruction and quantification were performed by using Huygens Essential Software.

DISCUSSION

This work explored the molecular and structural changes during the adaptation of the secretory pathway to high secretory demand. We used a thyroid cell line that physiologically responds to TSH to induce the synthesis of thyroid-specific cargo proteins, such as thyroglobulin and NIS, that require the secretory pathway to reach

Journal of Cell Science (2017) 130, 4155-4167 doi:10.1242/jcs.211102

their final destination. Immunofluorescence and western blots data indicate that the TSH stimulus increases levels of the thyroid-specific cargo protein NIS as well as that of transport factors localized to distinct compartments of the secretory pathway. Among these are the ER-localized chaperones, calreticulin and calnexin, which have been previously shown to be upregulated in thyrocytes stimulated with TSH and during the differentiation of resting B cells into antibody-secreting plasma cells (Christis et al., 2010; van Anken et al., 2009). Levels of Golgi-localized transport factors also increased in response to TSH and correlated with increased mRNA levels, suggesting that TSH induces a transcriptional regulation program required for cellular adaptation to a high secretory demand. These data are in agreement with a microarray analysis performed in FRTL-5 cells stimulated with TSH that showed an increase in mRNAs encoded by two genes required for vesicle transport, syntaxin 7 and the Golgi-associated protein GCP360 (also known as GOLGB1) (Calebiro et al., 2006).

The stimulatory effects of TSH on the expression of cargo protein and transport factors were similar to those observed when cellular adenylate cyclase was directly stimulated with forskolin. The ability of forskolin to mimic the TSH effects indicates that a cAMP-mediated pathway is responsible for the transcriptional amplification of genes encoding cargo proteins and transport factors, and suggested the involvement of a CRE motif in the response. In support, a comparative promoter region analysis showed that the CREB3L1 consensus sequence was highly enriched in 32 analyzed transport factors. This sequence is similar to that of the ATF/CREs (Hai and Hartman, 2001), as well as that of the UPR element (UPRE) (Schröder and Kaufman, 2005). Moreover, this sequence is related to the binding consensus motif of the *Drosophila* CrebA transcription factor, which is required and sufficient for the upregulation of numerous secretory pathway component genes in the developing salivary gland (Fox et al., 2010). Interestingly, while basal secretion in all cells appears to be independent of CrebA, its functions are essential in specialized secretory cells challenged with an increased need for cargo trafficking. Analysis of TSH effects on the mRNA levels of CREB3 isoforms showed that there was a significant increase in CREB3L1 mRNA, but not mRNA encoding other CREB3 family members (CREB3, CREB3L2, CREB3L3 and CREB3L4), suggesting that CREB3L1 is a key mediator of the TSH activity in thyroid cells. However, it remains possible that other factor(s) also participate in the process. CREB3L1 protein levels progressively increased until 14 h of TSH stimulation and then returned to basal levels after 24 h of TSH stimulation. This modality could be because CREB3L1 acts as a regulator during the acute phase of the TSH response, and after cell adaptation, other factors regulate the long-term TSH response. Alternatively, CREB3L1 levels may fall faster than those of transport factors, which could have a longer half-life. Low levels of active CREB3L1 are present in cells without TSH stimulation, most likely due to the presence of other activating factors in the growth medium. Alternatively, low levels of CREB3L1 could be constitutively expressed in FRTL-5 cells.

Our data show that the increased synthesis of cargo and transport factors in response to TSH stimulation is associated with structural modifications in the size and complexity of the Golgi complex, a key station for post-translational modification of the vast majority of cargo proteins. Although changes in Golgi complex morphology in resting thyroid cells or during intense activity of the thyroid gland have been observed previously (Cramer and Ludford, 1926), the molecular mechanisms that mediate these changes are poorly understood. We show that the TSH stimulus led to a rapid (within hours) increase in Golgi volume, due to an increase in the number of cisternae per stack, increased cisternal length and cisternal dilation. Importantly, the TSH-induced Golgi expansion could be mimicked by expressing either the full-length CREB3L1 or the transcriptionally active N-terminal fragment of CREB3L1 in cells without TSH-stimulation. Moreover, both constructs potentiated the effect of TSH-induced effect, strongly suggesting that TSH mediates its effect through CREB3L1. This was further supported by the ability of a dominant-negative CREB3L1 construct to obstruct the Golgi volume increase in cells stimulated with TSH. To the best of our knowledge, the ability of CREB3L1 to induce morphological changes in the structure of the Golgi complex has not been reported before. In agreement with the increase in Golgi volume, TSH also increases the expression of the sterol responsive element-binding proteins (SREBP1 and SREBP2) (Ringseis et al., 2013), master transcriptional regulators of cholesterol and fatty acid synthesis necessary for increased membrane production. Taken together, our data show that CREB3L1 expression is sufficient to induce a program capable of inducing the expression of factors required for Golgi expansion in thyroid FRTL-5 cells.

Our study underscores the general function of the CrebA/CREB3-like factors in coordinating the production of cargo proteins that vary between cells and tissues (for example collagen in chondrocytes) with an increased production of ubiquitous transport factors conserved in all cells. It is perhaps not surprising that the CrebA/CREB3-like transcriptional regulation is highly conserved within the evolutionary tree, between cell types, and across multiple varying types of induction stimuli, since the machinery mediating secretion is also highly conserved in all eukaryotes.

Our studies highlight the general role of the CrebA/CREB3-like transcription factors as major and direct coordinators of secretory demand and capacity irrespective of the induction stimulus. While previous work documented the role of CrebA/CREB3-like transcription factors during a long-term developmental program related to differentiation (Chan et al., 2011; Fox and Andrew, 2015), our results show their involvement in the secretory response induced by an acute hormonal stimulation. The similarity or difference in the signaling pathways involved in the response to different types of secretion stimuli and the correlation between CREB3L1 regulation and its impact on thyroid function in health and disease remain to be characterized.

MATERIALS AND METHODS

DNA constructs and antibodies

CREB3L1FL construct and CREB3L1CA and CREB3L1DN mutants were kindly supplied by Dr Deborah J. Andrew (The Johns Hopkins University, Baltimore, MD; Fox et al., 2010) and Dr David Murphy (University of Bristol, UK and University of Malaya, Malaysia; Greenwood et al., 2014).

The following primary antibodies were used: rabbit polyclonal antibodies to p115 (a gift from Dr Elizabeth Sztul, University of Alabama at Birmingham, Birmingham, AL; Nelson et al., 1998), NIS (a gift from Dr Nancy Carrasco, Yale University School of Medicine, New Haven, CT; Levy et al., 1997), Calreticulin (Affinity BioReagents, Golden, CO), Calnexin and Rab1b (catalog no. SC-6465 and SC-599, respectively, Santa Cruz Biotechnology, Santa Cruz, CA), GalNAcT2 and Sec23a (catalog no. HPA011222 and S7696, respectively, Sigma-Aldrich, St. Louis, MO), CREB3L1 and CREB3L2 (catalog no. ARP36109_T100 and ARP34673_T100, respectively, Aviva Systems Biology, San Diego, CA); Sec16a (catalog no. A300-648A, Bethyl laboratories, Montgomery): goat polyclonal antibody to CREB3L1 (catalog no. AF4080, R&D Systems, Minneapolis, MN); and mouse monoclonal antibodies to GM130 and GBF1 (catalog no. 610823 and 612116, respectively, BD Biosciences, San Jose, CA), golgin 97 (Molecular Probes, Eugene, OR), GAPDH (Ambion, USA) and Arf1 (Abcam, Cambridge, MA). The following secondary antibodies were used: goat anti-mouse-IgG conjugated to Alexa Fluor 594 or 488, goat

Journal of Cell Science (2017) 130, 4155-4167 doi:10.1242/jcs.211102

anti-rabbit-IgG conjugated to Alexa Fluor 488 or 594, donkey anti-mouse-IgG conjugated to Alexa Fluor 594, donkey anti-goat-IgG conjugated to Alexa Fluor 488 (Invitrogen, Carlsbad, CA), goat anti-mouse-IgG conjugated to horseradish peroxidase (HRP), goat anti-rabbit-IgG conjugated to HRP (Zymed, San Francisco, CA), goat anti-mouse-IgG conjugated to IRDye 800CW or 680RD and goat anti-rabbit-IgG conjugated to IRDye 800CW (LiCor Biosciences, Lincoln, NE).

Cell culture and transient transfections

The thyroid cell line FRTL-5 (ATCC CRL 8305; Van Heuverswyn et al., 1984) was grown in Dulbecco's modified Eagle's medium (DMEM)/F12 medium (Life Technologies, Grand Island, NY), supplemented with 5% newborn calf serum (GIBCO, Gaithersburg, MD), 1 mIU/ml bovine TSH (supplied by Dr Albert F. Parlow, National Institute of Diabetes and Digestive and Kidney Diseases, Torrance, CA), 10 µg/ml bovine insulin, 5 µg/ml bovine transferrine (Sigma-Aldrich, St. Louis, MO), and penicillin-streptomycin (GIBCO, Gaithersburg, MD) (denoted growth conditions). When cells reached 60–70% confluence, they were cultured for 72 h in the same medium but without TSH and containing 0.2% newborn calf serum (denoted basal condition, −TSH). TSH-starved cells were treated with 1 mIU/ml of TSH for different periods of time (stimulated condition, +TSH). Alternative, cells were treated with 10 µM forskolin (FSK, Sigma-Aldrich, St. Louis, MO).

FRTL-5 cells were transiently transfected in six-well multiwell plates by using Lipofectamine 2000 (Invitrogen, Carlsbad, CA) as specified by the manufacturer. At 24 h after transfection, cells were cultured for 36 h in basal conditions and then stimulated with 1 mIU/ml of TSH for different periods of time.

Immunofluorescence and image analysis

Immunofluorescence analysis was performed as described previously (Alvarez et al., 2003) using the following antibody dilutions: anti-Rab1b at 1:30; anti-GBF1 and Arf1 at 1:150; anti-GM130, Golgin97, GalNAcT2, Sec16a and Sec23a at 1:200; anti-CREB3L1 at 1:300; anti-p115 at 1:500; anti-Calreticulin and NIS at 1:1000; and secondary antibodies and Hoechst 33258 (cat. no. H-3569) (Molecular Probes, Eugene, OR) at 1:800.

Immunofluorescence was analyzed by using an optical microscope (Nikon eclipse TE2000-U, CIBICI-CONICET). To estimate Golgi size, confocal image sets obtained with an Olympus FluoView 300 confocal microscope (Sistema Nacional de Microscopía, Argentina) were used to determine the volume of the staining corresponding to the Golgi markers GM130 and GalNAcT2. Sections at 0.15-µm spacing were acquired. The Huygens Essential software was used for spatial deconvolution, three-dimensional reconstruction and quantification. Individual Golgi complexes were selected with the free-hand tool, and their volumes were determined by using the 'analyze particles' function. Cell size was estimated by performing flow cytometry for each condition, setting the cell size at 0 h as one; Golgi volume was normalized to the relative cell size value at each time point. In this way, results are independent of possible cell size variations.

Western blotting

For preparation of whole-protein extracts, FRTL-5 cells were washed with phosphate-buffered saline (PBS), collected with trypsin and rinsed with DMEM/F12 medium and PBS. Cells were pelleted and suspended in RIPA buffer containing protease inhibitors (catalog no. 11873580001, Roche Diagnostics, Indianapolis, IN) for 30 min on ice, and then centrifuged at 13,000 ***g*** for 20 min. Supernatants were separated by SDS-PAGE, and proteins were transferred to a nitrocellulose membrane (Thermo Scientific, Waltham, MA). Ponceau staining was used to verify protein transference to the membrane. The membrane was blocked in Tris-buffered saline with 0.1% Tween 20 (TBS-T) with 5% nonfat dried milk powder for 1 h at room temperature or at overnight at 4°C according to the antibody used. Blots were incubated with primary antibodies diluted in TBS-T with 5% nonfat dried milk powder overnight at 4°C, except when using anti-GAPDH and anti-calreticulin antibodies, which were incubated for 1 h at room temperature. After washing with TBS-T and TBS, the blots were incubated with HRP-conjugated secondary antibodies diluted in TBS-T with 5% nonfat dried milk powder (1:5000) at room temperature for 1 h. Protein–antibody complexes were visualized using chemiluminescence detection system (SuperSignalWest Pico; Pierce) and exposed to X-ray film (Kodak, Rochester, NY) or high-performance chemiluminescence film (GE Healthcare, Little Chalfont, UK). Alternatively, after primary antibody incubation, the blots were incubated with IRDye-conjugated secondary antibodies diluted in TBS-T (1:10,000) at room temperature for 1 h. Infrared signals were detected and analyzed with an OdysseyClx System (LiCor Biosciences) through the Image Studio Software. The following primary antibody dilutions were used: anti-Rab1b at 1:100; anti-GM130, Golgin97, GBF1 and Arf1 at 1:250; anti-CREB3L1 and CREB3L2 at 1:700; anti-p115 at 1:1000; anti-Sec23a at 1:2000; anti-calreticulin, calnexin and NIS at 1:1000; and anti-GAPDH at 1:12,000. For western blot quantification, the intensity of each band normalized to GAPDH or to tubulin (loading controls) was measured, and the fold change was calculated as the ratio of the normalized values in the TSH-induced (+TSH) versus the non-induced (−TSH) or control sample. Unless indicated, three independent experiments were performed and each sample was run in duplicate. The normalized value of one control was set as one, the other values of the controls were calculated relative to this values, and average values are shown in the bar graphs. Therefore, the values in the different control conditions are close to one and their error bars represent ±s.e.m.

RNA isolation and qRT-PCR

Total RNA was purified from FRTL-5 cells by using Trizol reagent (Invitrogen, Carlsbad, CA) according to the manufacturer's protocol. Synthesis of cDNA was performed from 1 µg of total RNA in a total volume of 20 µl using random primers (Invitrogen, Carlsbad, CA) and 50 U M-MLV reverse transcriptase (Promega, Madison, WI).

Primers were manually designed with the assistance of the Netprimer software (PREMIER Biosoft International, Palo Alto, CA). Primers were from Sigma-Genosys (Houston, TX) or Macrogen (Seoul, Korea), and their concentrations and sequences (5′–3′) are: β-actin (333,3 nM), GGCA CCACACTTTCTACAATG (F), TGGCTGGGGTGTTGAAGGT (R); NIS (333,3 nM), GCTGTGGCATTGTCATGTTC (F), TGAGGTCTT CCACAGTCACA (R); TG (333,3 nM), GAATTGCTGGCAGATGTTC AG (F), GGGCACTGAGCTCCTTGTAG (R); Sec31a (150 nM), ATTCGGAGGGAAGTTGGTGAC (F), TCTGAGCGGCTGAGGAAG TC (R); GM130 (150 nM), CGGGATGTCGGAAGAAAC (F), GTGT GGTCTGTGGGCACATT (R), Rab1b (250 nM) AACGGTTCAGG ACCATCACTTC (F) TCTCACTGGCGTAGCGATCTATT (R); KDELR3 (100 nM), GGCATCTCTGGGAAGAGTCAG(F), ATAGGCAC ACAGGAGGAAAACC (R); CREB3L1 (300 nM), GTGAAAGAAGA CCCCGTCGC (F), CTCCACAGGCAGTAGAGCACC (R); CREB3L2 (300 nm), CGGGCTCAGTCACCATTTACC (F) CCATTTCTCACTCT CCACCTCC (R); CREB3 (200 nM), GGAAAGTGGAGATTT GTGGGC (F), GCACGGAGTTCTCGGAAG (R); CREB3L3 (300 nM), TCCAGTGCGAGTGTTTTCCA (F), CAGAAGAGCCTTTGTGGGGT (R); CREB3L4 (300 nM), TGGAGAGGCAGAACATCTCGT (F), CTGGGCAGGATGATGAGAGC (R). qPCR analysis was performed by using an ABI Prism 7500 detection system (Applied Biosystems, Foster City, CA) and SYBR Green chemistry. Reactions were carried out in triplicate using 1× SYBR Green PCR Master Mix (Applied Biosystems) in a total volume of 15 µl. Specificity was verified by melting curve analysis and agarose gel electrophoresis. The fold change in gene expression was calculated according to the $2^{-\Delta\Delta Ct}$ method using β-actin as the internal control (Livak and Schmittgen, 2001).

Transmission electron microscopy

FRTL-5 cells were washed with PBS and centrifuged (500 ***g*** for 5 min) to obtain a visible pellet. Cells were than fixed with a 1% glutaraldehyde and 0.2 M Hepes. After dehydration, thin sections from each sample were cut with a Leica EM UC7 ultramicrotome and further investigated using a FEI Tecnai-12 (FEI, Eindhoven, The Netherlands) electron microscope equipped with a Veletta CCD camera for digital image acquisition at different magnifications.

Cell cytometry

We analyzed cells size by using a dot plot graphic of the FSC (forward scatter) against the SSC (side scatter) parameter, as obtained through flow

cytometry measurements, of the total cell population in control cells (–TSH) versus cells stimulated with TSH. The comparison of the mean of the FSC and SSC of both cell populations did not show any significant changes in the average cell size or cell complexity after incubation of cells with TSH, indicating that both cell populations are alike. Cells were acquired in a FACSCanto II flow cytometer and analyzed by using FlowJo software (Tree Star, Ashland, OR).

shRNA

We inhibited CREB3L1 expression by using a commercial pGFP-C-shLenti vector (Origene, Rockville, MD). This vector was designed to inhibit CREB3L1 expression (5′-GCCACCGAGGTGCTCTACTGCCTGTGG AG-3′) and also encode the GFP protein as a marker of transfection. Cells were transiently transfected with this vector, and 48–72 h after transfection, GFP-expressing cells were isolated by fluorescence-activated cell sorting (FACS). An equivalent treatment was performed on cells transfected with a control vector with a shRNA control cassette.

Statistical analysis

Results are presented as the mean±s.e.m. of at least three independent experiments performed in duplicates or triplicates. Comparisons between two groups were made by using an unpaired Student's *t*-test. Multiple group analysis was conducted by one-way ANOVA. As a post-test, the Bonferroni multiple-comparisons test was used. Statistical tests were performed by using the GraphPad Prism 5.0 software (GraphPad Software, San Diego, CA). Differences were considered significant at $P<0.05$.

Acknowledgements

The authors thank Hector A. Saka (Universidad Nacional de Córdoba, Córdoba, Argentina) for his comments after reading the manuscript. We thank Drs Carlos Mas, Cecilia Sampedro for microscope technical assistance, and Paula Abadie and Pilar Crespo for cell cytometry technical assistance. We also thank Drs Javier Jaldin and Graciela Panzetta (Universidad Nacional de Córdoba, Córdoba, Argentina) for helping with deconvolution and qRT-PCR analysis, respectively. Microscopes used in this work belong to the 'Centro de Microscopía Optica y Confocal de Avanzada' (CIQUIBIC, INIMEC, CIBICI)-CONICET-Universidad Nacional de Córdoba, Córdoba, Argentina.

Competing interests

The authors declare no competing or financial interests.

Author contributions

Conceptualization: I.A.G., C.A.; Methodology: I.A.G., V.T.D., D.V., P.D.G., Y.E., R.S. P., L.S., H.M.; Software: D.V.; Validation: I.A.G., D.V., P.D.G., Y.E., C.A.; Formal analysis: I.A.G., P.D.G., Y.E., L.S., C.A.; Investigation: I.A.G., V.T.D., L.S., C.A.; Resources: L.S.; Data curation: I.A.G., V.T.D., H.M.; Writing - original draft: I.A.G., V.T.D., E.S., C.A.; Writing - review & editing: R.S.P., E.S., C.A.; Visualization: I.A.G., R.S.P., C.A.; Supervision: R.S.P., C.A.; Project administration: C.A.; Funding acquisition: C.A.

Funding

This work was supported by Consejo Nacional de Investigaciones Científicas y Técnicas (CONICET), Fondo para la Investigación Científica y Tecnológica (FONCYT) (Préstamo BID 2012. PICT 0043), and Secretaría de Ciencia y Técnica, Universidad Nacional de Córdoba (Secyt UNC) to C.A. as principle investigator. Secyt UNC, CONICET, FONCYT and Instituto Nacional de Cáncer (INC) granted fellowships to I.A.G, V.T.D., L.S. and H.M., respectively. C.A. is member of CONICET.

Supplementary information

Supplementary information available online at
http://jcs.biologists.org/lookup/doi/10.1242/jcs.211102.supplemental

References

Abrams, E. W. and Andrew, D. J. (2005). CrebA regulates secretory activity in the Drosophila salivary gland and epidermis. *Development* **132**, 2743-2758.

Alvarez, C., Garcia-Mata, R., Brandon, E. and Sztul, E. (2003). COPI recruitment is modulated by a Rab1b-dependent mechanism. *Mol. Biol. Cell* **14**, 2116-2127.

Bailey, D. and O'Hare, P. (2007). Transmembrane bZIP transcription factors in ER stress signaling and the unfolded protein response. *Antioxid Redox Signal.* **9**, 2305-2321.

Barbosa, S., Fasanella, G., Carreira, S., Llarena, M., Fox, R., Barreca, C., Andrew, D. and O'Hare, P. (2013). An orchestrated program regulating secretory pathway genes and cargos by the transmembrane transcription factor CREB-H. *Traffic* **14**, 382-398.

Bonfanti, L., Mironov, A. A., Jr, Martínez-Menárguez, J. A., Martella, O., Fusella, A., Baldassarre, M., Buccione, R., Geuze, H. J., Mironov, A. A. and Luini, A. (1998). Procollagen traverses the Golgi stack without leaving the lumen of cisternae: evidence for cisternal maturation. *Cell* **95**, 993-1003.

Calebiro, D., de Filippis, T., Lucchi, S., Martinez, F., Porazzi, P., Trivellato, R., Locati, M., Beck-Peccoz, P. and Persani, L. (2006). Selective modulation of protein kinase A I and II reveals distinct roles in thyroid cell gene expression and growth. *Mol. Endocrinol.* **20**, 3196-3211.

Cancino, J., Capalbo, A., Di Campli, A., Giannotta, M., Rizzo, R., Jung, J. E., Di Martino, R., Persico, M., Heinklein, P., Sallese, M. et al. (2014). Control systems of membrane transport at the interface between the endoplasmic reticulum and the Golgi. *Dev. Cell* **30**, 280-294.

Capitani, M. and Sallese, M. (2009). The KDEL receptor: new functions for an old protein. *FEBS Lett.* **583**, 3863-3871.

Chan, C.-P., Kok, K.-H. and Jin, D.-Y. (2011). CREB3 subfamily transcription factors are not created equal: recent insights from global analyses and animal models. *Cell Biosci* **1**, 6.

Christis, C., Fullaondo, A., Schildknegt, D., Mkrtchian, S., Heck, A. J. R. and Braakman, I. (2010). Regulated increase in folding capacity prevents unfolded protein stress in the ER. *J. Cell Sci.* **123**, 787-794.

Clermont, Y., Xia, L., Rambourg, A., Turner, J. D. and Hermo, L. (1993). Structure of the Golgi apparatus in stimulated and nonstimulated acinar cells of mammary glands of the rat. *Anat. Rec.* **237**, 308-317.

Cramer, W. and Ludford, R. J. (1926). On cellular activity and cellular structure as studied in the thyroid gland. *J. Physiol.* **61**, 398-408.

Dremier, S., Coulonval, K., Perpete, S., Vandeput, F., Fortemaison, N., Van Keymeulen, A., Deleu, S., Ledent, C., Clément, S., Schurmans, S. et al. (2002). The role of cyclic AMP and its effect on protein kinase A in the mitogenic action of thyrotropin on the thyroid cell. *Ann. N. Y. Acad. Sci.* **968**, 106-121.

Fox, R. M. and Andrew, D. J. (2015). Transcriptional regulation of secretory capacity by bZip transcription factors. *Front. Biol.* **10**, 28-51.

Fox, R. M., Hanlon, C. D. and Andrew, D. J. (2010). The CrebA/Creb3-like transcription factors are major and direct regulators of secretory capacity. *J. Cell Biol.* **191**, 479-492.

Fromme, J. C., Orci, L. and Schekman, R. (2008). Coordination of COPII vesicle trafficking by Sec23. *Trends Cell Biol.* **18**, 330-336.

Garcia-Mata, R., Szul, T., Alvarez, C. and Sztul, E. (2003). ADP-ribosylation factor/COPI-dependent events at the endoplasmic reticulum-Golgi interface are regulated by the guanine nucleotide exchange factor GBF1. *Mol. Biol. Cell* **14**, 2250-2261.

Greenwood, M., Bordieri, L., Greenwood, M. P., Rosso Melo, M., Colombari, D. S. A., Colombari, E., Paton, J. F. R. and Murphy, D. (2014). Transcription factor CREB3L1 regulates vasopressin gene expression in the rat hypothalamus. *J. Neurosci.* **34**, 3810-3820.

Hai, T. and Hartman, M. G. (2001). The molecular biology and nomenclature of the activating transcription factor/cAMP responsive element binding family of transcription factors: activating transcription factor proteins and homeostasis. *Gene* **273**, 1-11.

Hughes, H. and Stephens, D. J. (2008). Assembly, organization, and function of the COPII coat. *Histochem. Cell Biol.* **129**, 129-151.

Levy, O., Dai, G., Riedel, C., Ginter, C. S., Paul, E. M., Lebowitz, A. N. and Carrasco, N. (1997). Characterization of the thyroid Na+/I- symporter with an anti-COOH terminus antibody. *Proc. Natl. Acad. Sci. USA* **94**, 5568-5573.

Livak, K. J. and Schmittgen, T. D. (2001). Analysis of relative gene expression data using real-time quantitative PCR and the 2(−Delta Delta C(T)) Method. *Methods* **25**, 402-408.

Morshed, S. A., Latif, R. and Davies, T. F. (2009). Characterization of thyrotropin receptor antibody-induced signaling cascades. *Endocrinology* **150**, 519-529.

Murakami, T., Saito, A., Hino, S., Kondo, S., Kanemoto, S., Chihara, K., Sekiya, H., Tsumagari, K., Ochiai, K., Yoshinaga, K. et al. (2009). Signalling mediated by the endoplasmic reticulum stress transducer OASIS is involved in bone formation. *Nat. Cell Biol.* **11**, 1205-1211.

Nelson, D. S., Alvarez, C., Gao, Y.-S., García-Mata, R., Fialkowski, E. and Sztul, E. (1998). The membrane transport factor TAP/p115 cycles between the Golgi and earlier secretory compartments and contains distinct domains required for its localization and function. *J. Cell Biol.* **143**, 319-331.

Ringseis, R., Rauer, C., Rothe, S., Gessner, D. K., Schütz, L.-M., Luci, S., Wen, G. and Eder, K. (2013). Sterol regulatory element-binding proteins are regulators of the NIS gene in thyroid cells. *Mol. Endocrinol.* **27**, 781-800.

Romer, K. A., Kayombya, G.-R. and Fraenkel, E. (2007). WebMOTIFS: automated discovery, filtering and scoring of DNA sequence motifs using multiple programs and Bayesian approaches. *Nucleic Acids Res.* **35**, W217-W220.

Romero, N., Dumur, C. I., Martinez, H., Garcia, I. A., Monetta, P., Slavin, I., Sampieri, L., Koritschoner, N., Mironov, A. A., De Matteis, M. A. et al. (2013). Rab1b overexpression modifies Golgi size and gene expression in HeLa cells and modulates the thyrotrophin response in thyroid cells in culture. *Mol. Biol. Cell* **24**, 617-632.

Journal of Cell Science

Ron, D. and Walter, P. (2007). Signal integration in the endoplasmic reticulum unfolded protein response. *Nat. Rev. Mol. Cell Biol.* **8**, 519-529.
Rottger, S., White, J., Wandall, H. H., Olivo, J. C., Stark, A., Bennett, E. P., Whitehouse, C., Berger, E. G., Clausen, H. and Nilsson, T. (1998). Localization of three human polypeptide GalNAc-transferases in HeLa cells suggests initiation of O-linked glycosylation throughout the Golgi apparatus. *J. Cell Sci.* **111**, 45-60.
Saito, A., Kanemoto, S., Zhang, Y., Asada, R., Hino, K. and Imaizumi, K. (2014). Chondrocyte proliferation regulated by secreted luminal domain of ER stress transducer BBF2H7/CREB3L2. *Mol. Cell* **53**, 127-139.
Schröder, M. and Kaufman, R. J. (2005). The mammalian unfolded protein response. *Annu. Rev. Biochem.* **74**, 739-789.
Seamon, K. B., Padgett, W. and Daly, J. W. (1981). Forskolin: unique diterpene activator of adenylate cyclase in membranes and in intact cells. *Proc. Natl. Acad. Sci. USA* **78**, 3363-3367.
Sengupta, D. and Linstedt, A. D. (2011). Control of organelle size: the Golgi complex. *Annu. Rev. Cell Dev. Biol.* **27**, 57-77.
Shaywitz, A. J. and Greenberg, M. E. (1999). CREB: a stimulus-induced transcription factor activated by a diverse array of extracellular signals. *Annu. Rev. Biochem.* **68**, 821-861.
Sinowatz, S., Wrobel, K. H., El Etreby, M. F. and Sinowatz, F. (1980). On the ultrastructure of the canine mammary gland during pregnancy and lactation. *J. Anat.* **131**, 321-332.
Sztul, E. and Lupashin, V. (2009). Role of vesicle tethering factors in the ER-Golgi membrane traffic. *FEBS Lett.* **583**, 3770-3783.
Szul, T. and Sztul, E. (2011). COPII and COPI traffic at the ER-Golgi interface. *Physiology* **26**, 348-364.
Trucco, A., Polishchuk, R. S., Martella, O., Di Pentima, A., Fusella, A., Di Giandomenico, D., San Pietro, E., Beznoussenko, G. V., Polishchuk, E. V., Baldassarre, M. et al. (2004). Secretory traffic triggers the formation of tubular continuities across Golgi sub-compartments. *Nat. Cell Biol.* **6**, 1071-1081.
van Anken, E., Pena, F., Hafkemeijer, N., Christis, C., Romijn, E. P., Grauschopf, U., Oorschot, V. M. J., Pertel, T., Engels, S., Ora, A. et al. (2009). Efficient IgM assembly and secretion require the plasma cell induced endoplasmic reticulum protein pERp1. *Proc. Natl. Acad. Sci. USA* **106**, 17019-17024.
Van Heuverswyn, B., Streydio, C., Brocas, H., Refetoff, S., Dumont, J. and Vassart, G. (1984). Thyrotropin controls transcription of the thyroglobulin gene. *Proc. Natl. Acad. Sci. USA* **81**, 5941-5945.
Zambelli, F., Pesole, G. and Pavesi, G. (2009). Pscan: finding over-represented transcription factor binding site motifs in sequences from co-regulated or co-expressed genes. *Nucleic Acids Res.* **37**, W247-W252.